



A perceptual stereoscopic image quality assessment model accounting for binocular combination behavior[☆]



Jiachen Yang^{a,1}, Yun Liu^{a,*,2}, Zhiqun Gao^a, Rongrong Chu^a, Zhanjie Song^b

^a School of Electronic Information Engineering, Tianjin University, China

^b School of Science, Tianjin University, China

ARTICLE INFO

Article history:

Received 29 December 2014

Accepted 2 June 2015

Available online 20 June 2015

Keywords:

Binocular vision

Image quality

Local amplitude

Gain control

Stereoscopic quality assessment

Difference channel

Summation channel

Symmetric distortion

ABSTRACT

Stereoscopic image quality assessment (SIQA) plays an important role in the development of 3D image processing. In this paper, a full-reference object SIQA model is built based on binocular summation channel and binocular difference channel. In our frame work, binocular combination behavior and how to experience the depth perception are thought to be the key factors to evaluate the quality of stereoscopic images. Differing from the current depth map methods, this method focuses on a new aspect, and an effective combination model is proposed based on the physiological findings in the Human Visual System (HVS). Experimental results demonstrate that the proposed quality assessment metric significantly outperforms the existing metrics and can achieve higher consistency with subject quality assessment when predicting the quality of stereoscopic images that have been symmetrically distorted.

© 2015 Elsevier Inc. All rights reserved.

1. Introduction

With the development of 3D technologies, more and more 3D contents for 3DTV and 3D cinema are produced. Being able to provide a high-quality 3D image and deliver to the consumer is both challenge and demanding. Differ from traditional 2D image quality assessment (2D-IQA) [1–3], many factors, such as depth perception, views' quality, and visual fatigue, could affect 3D perception. How to evaluate the quality of stereoscopic image quality draw much attention.

Many efforts have already been done to develop stereoscopic image quality assessment method (SIQA) over the last decade which can be categorized into two types: the subjective and objective models. Since subjective SIQA is time-consuming and impractical for online applications, the objective SIQA has been a fruitful area of work. In the past years, many researchers directly applied 2D-IQA metrics to measure 3D perception [4,5]. However, these methods based on 2D-IQA performed poorly in predicting the quality of stereoscopic images, since these metric were failed in considering strong correlation with standard disparity from two adjacent

viewpoints. It shown that the perceptual quality of stereoscopic images cannot be predicted by simply averaging the quality of the left and right image. Hence, it is very necessary to develop an effective method to evaluate the objective quality of stereoscopic images.

Recently, a considerable amount of research have been conducted on SIQA [6,7]. Various factors that may affect the degree of visual comfort experience have been found and studied [8,9]. Considering that the depth information is the big difference between 2D image and stereoscopic images, many SIQA models have been proposed. For example, Benoit et al. [10] presented a linear combination of the disparity map distortion and the measure of the 2D image quality on both eyes. Lambooi et al. [11] proposed a 3D quality model by considering 2D image quality and perceived depth. Some other works have been conducted based on human visual perception. Kim et al. [12] proposed a visual fatigue prediction metric which can replace subjective evaluation for stereoscopic images. Chen et al. [13] explored a SIQA model by considering the image quality, depth quality and visual comfort. However, the above models needed to assess the depth quality using estimated disparity maps, and the ground truth disparity or depth is generally not available. The performance of the related SIQA model would be substantially affected by the accuracy of the used disparity estimation algorithm.

Later, many SIQA models based on HVS to stimulate binocular characteristics were proposed. Shao et al. [14] proposed a perceptual full-reference SIQA model by considering the binocular visual characteristics. Chen et al. [15] addressed binocular rivalry issues

[☆] This paper has been recommended for acceptance by M.T. Sun.

* Corresponding author.

E-mail address: yunliu@tju.edu.cn (Y. Liu).

¹ In 2014, he is a visiting scholar in the Department of Computer Science, Loughborough University, United Kingdom.

² Now she is a visiting Ph.D. student in University of California at Berkeley.

by modeling the binocular suppression behaviors and developed a framework for assessing the quality of 3D images. Lin et al. [16] integrated the binocular integration behaviors, the binocular combination and the binocular frequency integration, into the existing 2D objective metrics for evaluating the quality of 3D images. These models were proposed by building a possible model of human binocular processing procedure when human viewing 3D content. The overall performance of these metrics indeed outperforms that of the former metrics in predicting the quality of stereoscopic images across different types of distortions. Remarkable progresses have been obtained in both theoretical and practical understanding about binocular perception of stereoscopic image [17,18]. What is more, with the development of human 3D visual system [19–21], more and more 3D visual quality assessment methods were proposed [22,23]. Tsai et al. [24] and Bosc et al. [25] proposed the quality assessment models of 3D synthesized views in the context of multi-view video, which enhances the correlation of the objective quality score to the 3D subjective scores. Later, Jiang et al. [26] proposed a 3D visual attention model for stereoscopic image quality assessment task, and the proposed 3D visual attention-based pooling scheme can achieve higher consistency with the subjective assessment of stereoscopic images. Battisi et al. [27] built an effective objective quality assessment model to evaluate the visual quality of DIBR-synthesized views. Park et al. [28] then developed an effective 3D visual discomfort predictor to predict the level of visual discomfort.

In this paper, a full reference quality assessment metric is proposed by applying properties of human binocular visual system. We take steps based on the biologically plausible visual processing which contains two channels: difference and summation channels. The principal advantage of this model is that we apply the absolute disparity to directly reflect human stereo sense instead of disparity map, which greatly reduce the algorithm complexity. Since the summation channel signal intrinsically reflect the image quality of 3D images, the proposed method of combining difference channel and summation channel (SDM) attains more accurate quality assessment.

The rest of this paper is organized as follows. Section 2 introduces some binocular combination models. The framework of the proposed metric is presented in Section 3. The experimental results are analyzed in Section 4, and finally conclusions are drawn in Section 5.

2. Binocular combination behavior

Human binocular vision is a complex visual process, and one of the most amazing properties of human binocular characteristics is the fusion of the left and right views of a scene into a 3D image. A large number of researches have been done on how two slightly different monocular images fuse to a “combined image” and generate depth perception.

2.1. Monocular channel

Traditionally, it is thought that the depth perception was achieved by simply combining the monocular information [29]. In 1968, Levelt [30] proposed a linear model to explain the perceived combination image when a stereoscopic image is present, as follows:

$$C = W_l \times E_l + W_r \times E_r \quad (1)$$

where C is the simulated cyclopean combined image, E_l and E_r are the signals from the left and right eyes, respectively. W_l and W_r are the weighting coefficients for the two eyes, respectively, where $W_l + W_r = 1$. Cogan et al. [31] then proposed a gain control model

to stimulate human binocular visual experience, as shown in Fig. 1. They stated that each eye would exerts gain control on the other eye, not just simply added together, the model is given by:

$$C = \frac{1}{1 + G_r} E_l + \frac{1}{1 + G_l} E_r \quad (2)$$

where G_l and G_r are the visually weight for gain control of the left and right images, respectively.

With the further development of vision model, numerous biological models were proposed to describe binocular combination (e.g. vector summation model shown in Eq. (3), and neural network model shown in Eq. (4)). The detailed description and comparisons can be found in the study of [32].

$$C = N_l + N_r \quad (3)$$

where N_l and N_r are the responses of neural cells receiving strong excitation to one eye and weak inhibition from the other eye, respectively. As in work [32], we can apply E_l and E_r to calculate N_l and N_r , since E_l and E_r are mathematically equivalent ($i = l, r$).

$$C = \left(\frac{E_l}{E_l + E_r} \right) E_l + \left(\frac{E_r}{E_l + E_r} \right) E_r \quad (4)$$

2.2. Binocular summation and difference channels

An alternative view, however, seems more plausible. It proposed that there exist “Summation” and “Difference” channels used for stereopsis. Indeed, Silva et al. [33] demonstrated such mechanisms exist and accounted for binocular brightness perception. What is more, Li and Atick [34] presented the existence of a visual pathway of binocular visual system (shown in Fig. 2). They pointed that the signals from the left and right eyes will be firstly transformed into two uncorrelated signals: Summation (S) and Difference signals D , and then gains, G_+ and G_- , applied to the summation and difference channels dynamically optimized to the prevailing interocular correlation, respectively. Recently, Kingdom et al. [35], in detail, explained the theory procedure of summation and difference channel and how these two channels added and subtracted the neural signals from our two eyes.

Given the left image L and right image R , the binocular S and D signals can be calculated based on Eq. (5), shown as follows:

$$\begin{cases} D = |L - R| \\ S = L + R \end{cases} \quad (5)$$

Here, we present an example, in Fig. 3, to show the human binocular summation and difference signal experience. The first row shows the left images of the reference stereoscopic images and WN distorted stereoscopic images, respectively. The second row is

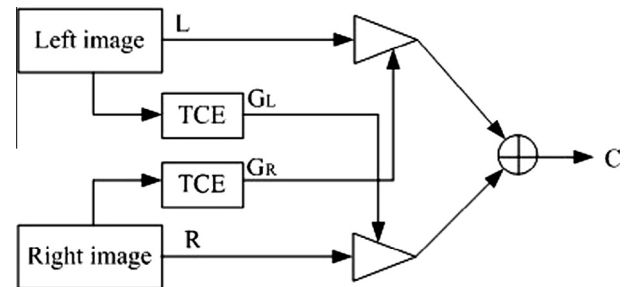


Fig. 1. The gain control model: Each eye exerts gain control on the other eye in proportion to its own total visually weighted contrast energy (TCE). Within a spatial-frequency-and-orientation channel, the input from each eye is divided by a gain-controlling signal from the other eye ($1 + \text{TCE}$) and the two dividends are summed linearly [31].

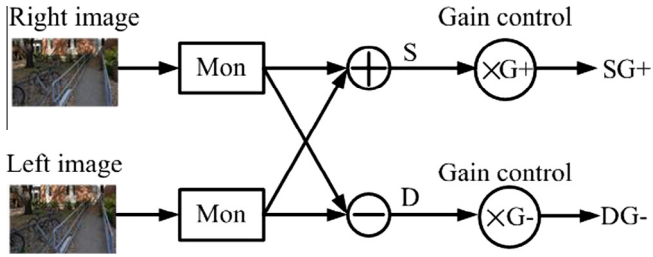


Fig. 2. The summation and difference channels: The signals from the left and right eyes are transformed into summation S and difference D signals. G_+ and G_- are the gains applied to summation and difference channels, respectively.

the reference Summation and Difference images of reference image shown in Fig. 3(a), while the last row is the distorted Summation and Difference images of distorted image shown in Fig. 3(b), respectively. It can be noticed that both Summation and Difference images can reflect the image quality, and some important image information are preserved in each of them, shown in Fig. 3(c)–(f). The Summation image presents more image quality information than Difference image, such as luminance, contrast and detail. While, as in work [36], the Difference image can be used to capture the directional reflection of human stereo sense. Based on the above discussion, the combination of Summation and Difference images could provide a more reasonable estimation of stereoscopic image quality.

Based on the above discussion, the proposed stereoscopic image quality assessment method will be built based on the Summation and Difference images by taking biological binocular model into consideration, which greatly reduced the computational complexity.

3. Proposed perceptual stereoscopic image quality assessment metric

As discussed in former sections, theory and model of the Summation and Difference signals can be validated to reflect certain physiological processes of human visual system, and can be used to evaluate the quality of stereoscopic images. With this inspiration, a full reference objective quality assessment model, SDM-M metric, for 3D images is built. The flowchart of our model is shown in Fig. 4.

3.1. Gain control processing

Qian et al. [37] proved that log-Gabors model could be well modeled human simple cells. Thus, we apply log-Gabors filters to calculate the local amplitude of Summation and Difference signals as the corresponding gain control, respectively. In our experiment, the design of the filter followed the work in [38]. Here we denote $[\eta_{s,o}, \zeta_{s,o}]$ as a set of responses on different scales and along different orientations, which can be obtained by applying the log-Gabor filter $G_{s,o}$ in the Fourier frequency domain:

$$G_{s,o}(\omega, \theta) = \exp \left[-\frac{(\log(\omega/\omega_s))^2}{2\sigma_s^2} \right] \times \exp \left[-\frac{(\theta - \theta_o)^2}{2\sigma_o^2} \right] \quad (6)$$

where s and o are spatial scale and orientation index, θ is the orientation angle, σ_s and σ_o determine the strength of the filter. ω and ω_s are the normalized radial frequency and the corresponding center frequency of the filter, respectively.

Based on the above analysis, we can get the local amplitude (A) at location X on different scale s along different orientation o :

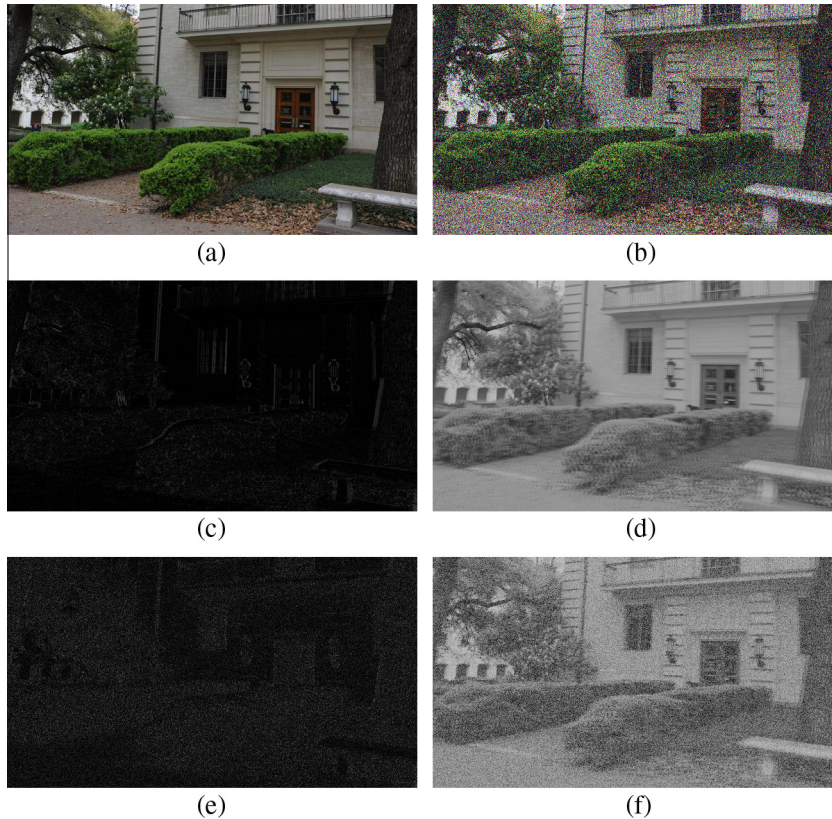


Fig. 3. (a) Left reference image. (b) Left distorted image. (c) The reference difference image. (d) The reference summation image. (e) The distorted difference image. (f) The distorted summation image.

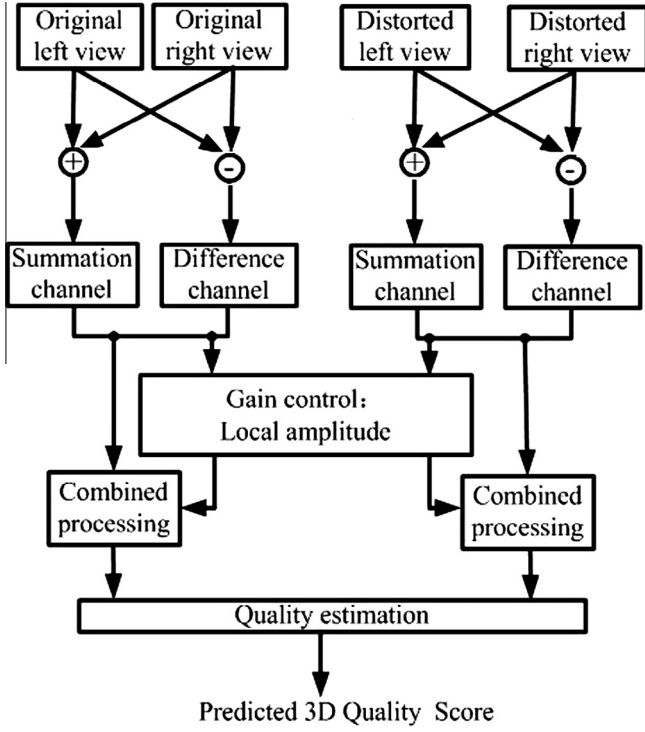


Fig. 4. The flowchart of the proposed stereoscopic image quality assessment metric.

$$A_{s,o}(X) = \sqrt{\eta_{s,o}(X)^2 + \zeta_{s,o}(X)^2} \quad (7)$$

The local energy along orientation o is given by:

$$E_o(X) = \sqrt{F_o(X)^2 + H_o(X)^2} \quad (8)$$

where $F_o(X) = \sum_s \eta_{s,o}(X)$ and $H_o(X) = \sum_s \zeta_{s,o}(X)$. Then the phase congruency $PC_o(X)$ along orientation o can be given by:

$$PC_o(X) = \frac{E_o(X)}{\varepsilon + \sum_s A_{s,o}(X)} \quad (9)$$

where ε is a small positive constant. In this work, the define of the local amplitude is followed by the work in [14], we can get the local amplitude based on the sum of local amplitude of all scales along the orientation o_m :

$$LA(X) = \sum_s A_{s,o_m}(X) \quad (10)$$

where o_m denotes the orientation which corresponds to the maximum phase congruency value: $PC_{o_m}(X) = \max PC_o(X)$.

3.2. Combination processing

Some interesting behaviors of binocular combination play an important role in selecting the plausible biological models of binocular combination (e.g. Fechner's paradox, cyclopean perception). Among the earlier researches, because the linear models, such as Vector Summation Model, Neural Network Model and Gain-Control Theory Model shown in Section 2, can well explain Fechner's paradox and cyclopean perception. Thus, we also adopt the linear model to stimulate the combination model.

As discussed earlier, stereopsis and the binocular combined image are achieved by Summation and Difference signals, but rather left and right images. The linear model of summation and difference signal with proper gains here is a natural way to stimulate a combined image. What is more, Li et al. [39] stated that as

long as the signal-to-noise ratio is not too low, this optimization amounts to equalization of the channel amplitudes. Thus, in this paper, we apply the local amplitude of a bank of log-Gabor filters as the gains to weight the summation and difference signal. The combined image can be given by:

$$C = A_{sum} \times S + A_{dif} \times D \quad (11)$$

where A_{sum} and A_{dif} are the corresponding local amplitude of summation and difference signals respectively, which are computed by log-Gabors filters.

3.3. Quality assessment metric

Finally, a full-reference 2D-IQA algorithm on the reference combination image and on the test combination image is expected to give a reasonable quality estimation of 3D image. The objective quality assessment value of a 3D image Q is given by:

$$Q = F(C_R, C_T) \quad (12)$$

where $F(\bullet)$ represents one of the 2D-IQA metrics (e.g. VIF [40], PSNR, GSSIM [41], MS-SSIM [42]). C_R and C_T are represent the reference and test combined image respectively. In general, we can define the corresponding SDM-M metric of each 2D metric on the basis of Eq. (12) (e.g. SDM-VIF shown in Eq. (13)).

$$Q_{SDM-VIF} = VIF(C_R, C_T) \quad (13)$$

4. Experiment result and analysis

4.1. Stereoscopic image quality database

In this experiment, we utilize the LIVE 3D image quality Database to verify the performance of our proposed SIQA model [43]. This database consists of 365 distorted images generated from 20 reference images, shown in Fig. 5, while Fig. 6 shows the processing images of one of them, including the Summation and Difference images, and the corresponding amplitude map of summation and difference images. Five types of distortion are applied to the reference images at various levels: (80 each for JP2K, JPEG, WN and FF; 45 for Blur) and all distortions are symmetric in nature. Each distorted image has a co-registered human score in the form of DMOS.

4.2. Performance measurement

Four consistency evaluation metrics are applied to measure the performance of the proposed SDM-M metric: Pearson linear correlation coefficient (PLCC), Spearman's rank ordered correlation coefficient (SROCC), Kendall rank-order correlation coefficient (KRCC), and the root-mean-squared error (RMSE). Higher PLCC, SROCC and KROCC indicated good correlation with human quality, while lower values of RMSE indicated better performance.

In order to evaluate the performance of the proposed scheme, we firstly compare SDM-M metrics with four 2D-IQA models, e.g., VIF, PSNR, GSSIM, MS-SSIM. Tables 1–4 show the consistency of all the above metrics with respect to the subjective MOS's, and the indicator highlighted in bold gives the best performance. Tables 1–4 demonstrate that 2D-IQA metrics perform poorly for evaluating the quality of 3D images, and our proposed SDM-M is better than these 2D-IQA metrics. Although some of 2D-IQA metrics achieve high performance (e.g. the PLCC and SROCC values of VIF, GSSIM and MS-SSIM are higher than 0.91), these methods do not take human visual system into consideration. Traditional 2D-IQA methods simply apply 2D-IQA algorithm on the left and right views and take the averaged value as the performance result.



Fig. 5. The 20 reference images (only left images are shown) used in the experiment.

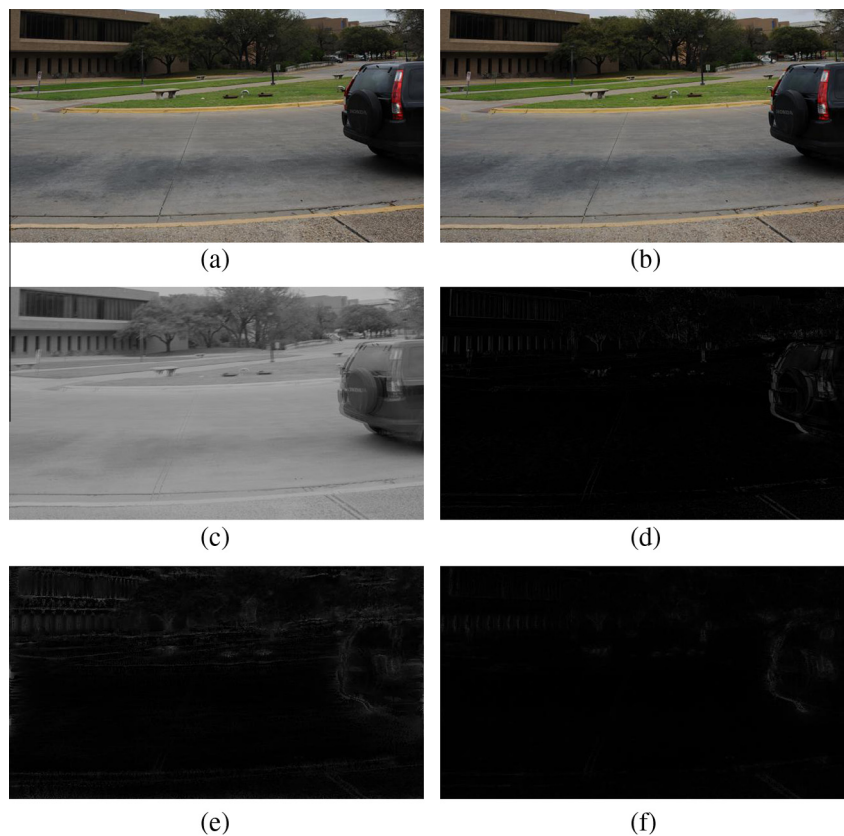


Fig. 6. (a) Left reference image. (b) right reference image. (c) Summation image. (d) Difference image. (e) The amplitude map of Summation image. (f) The amplitude map of Difference image.

Table 1

PLCC scores obtained by averaging left and right quality assessment scores (centering column) and using the SDM-metric.

| Molde | 2D model | SDM-M metric |
|---------|----------|---------------|
| VIF | 0.9249 | 0.9286 |
| PSNR | 0.8345 | 0.8405 |
| GSSIM | 0.9186 | 0.9332 |
| MS-SSIM | 0.9261 | 0.9311 |

Table 2

SROCC scores obtained by averaging left and right quality assessment scores (centering column) and using the SDM-metric.

| Molde | 2D model | SDM-M metric |
|---------|----------|---------------|
| VIF | 0.9200 | 0.9239 |
| PSNR | 0.8341 | 0.8355 |
| GSSIM | 0.9156 | 0.9284 |
| MS-SSIM | 0.9239 | 0.9268 |

Table 3

KRCC scores obtained by averaging left and right quality assessment scores (centering column) and using the SDM-M metric.

| Molde | 2D model | SDM-M |
|---------|----------|---------------|
| VIF | 0.7400 | 0.7476 |
| PSNR | 0.6297 | 0.6348 |
| GSSIM | 0.7361 | 0.7568 |
| MS-SSIM | 0.7487 | 0.7561 |

Table 4

RMSE scores obtained by averaging left and right quality assessment scores (centering column) and using the SDM-M metric.

| Molde | 2D model | SDM-M |
|---------|----------|---------------|
| VIF | 8.3153 | 8.1127 |
| PSNR | 12.0480 | 11.8446 |
| GSSIM | 8.6411 | 7.8572 |
| MS-SSIM | 8.2486 | 7.9773 |

Our proposed SDM-M metrics based on human binocular characteristics, improve the performance of all the 2D-IQA metrics. Besides, the results present that SDM-GSSIM has the outstanding performance among all the proposed SDM-M metrics. Fig. 7 breaks down the performance of the SDM-GSSIM. It also prove that the Summation and Difference signals are the important information in stereoscopic images which play an important role in image quality assessment, and our SDM-GSSIM successfully captures and utilizes these human binocular combination experience to predict image quality.

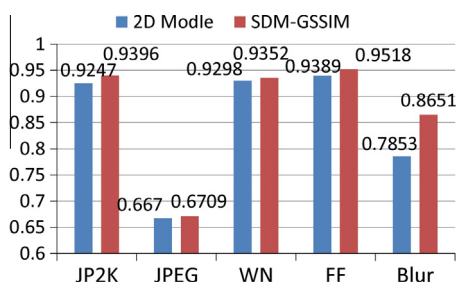


Fig. 7. PLCC values comparison between 2D model and SDM-GSSIM, broken down by distortion type.

To obtain deeper insights into the predict performance of the proposed SIQA-M metrics, we compare our method with three state-of-art SIQA schemes: Benoit's scheme [10], Chen's scheme [15] and Lin's scheme [16]. Since the SDM-GSSIM delivers the highest performance (see Tables 1–4), we use the SDM-GSSIM algorithm to compare with other schemes. To save space, here only the values of PLCC and RMSE of each distortion type with the LIVE 3D image quality Database are listed in Tables 5 and 6. The overall performance comparison among these SIQA schemes is presented in Table 7, where the indicator that gives the best performance is highlighted in bold. It clearly present that the proposed SDM-GSSIM metric outperforms other schemes.

To be more specific, for Benoit's scheme, they combine the image quality and disparity maps together based on 2D-IQA method, the overall assessment performance are not very good. Since Benoit's metric requires disparity information, the performance may be affected by the accuracy of the disparity calculation. The model of Chen is based on a plausible study of visual processing and apply an internal image instead of the true combined image, even though it may be effective for the individual distortion type (e.g. White Noise), the overall assessment performance is not very good. The reason is that uniform assessment is adopted for left and right images of different distortion types, and thus, poor convergence across different distortion types is occurred. For Lin's metric, it is proposed based on the binocular integration behaviors to measure the quality of stereoscopic 3D images. However, its overall performance is not very high, since it does not take the disparity information into consideration. The proposed SDM-GSSIM metric shows the higher overall performance than other models shown in Table 7. For each type of the distortion, the proposed SDM-GSSIM metric performs the best on the distortion of 'JP2K', 'JPEG', 'FF' and 'Blur', except for the distortion of 'WN', but the performance values is very close to the best one.

Table 5

PLCC performance comparison of various SIQA schemes (the cases in bold: the best performance) on LIVE 3D image quality database.

| Distortion | Benoit [10] | Chen [15] | Lin [16] | SDM-GSSIM |
|------------|-------------|---------------|----------|---------------|
| JP2K | 0.8897 | 0.9163 | 0.8381 | 0.9396 |
| JPEG | 0.5580 | 0.6344 | 0.2866 | 0.6709 |
| WN | 0.9360 | 0.9431 | 0.9280 | 0.9352 |
| Blur | 0.9256 | 0.9416 | 0.9475 | 0.9518 |
| FF | 0.7514 | 0.7574 | 0.7086 | 0.8650 |

Table 6

RMSE performance comparison of various SIQA schemes (the cases in bold: the best performance) on LIVE 3D image quality database.

| Distortion | Benoit [10] | Chen [15] | Lin [16] | SDM-GSSIM |
|------------|-------------|---------------|----------|---------------|
| JP2K | 7.8853 | 6.9137 | 9.4210 | 5.9086 |
| JPEG | 7.2354 | 6.7397 | 8.3531 | 6.4654 |
| WN | 7.8088 | 7.3733 | 8.2618 | 7.8532 |
| Blur | 7.3051 | 6.4964 | 6.1721 | 5.9188 |
| FF | 10.9314 | 10.8173 | 11.6895 | 8.3132 |

Table 7

The overall performance comparison among various 3D SIQA schemes on LIVE 3D image quality database.

| Criteria | Benoit [10] | Chen [15] | Lin [16] | SDM-GSSIM |
|----------|-------------|-----------|----------|---------------|
| PLCC | 0.8829 | 0.9167 | 0.8645 | 0.9332 |
| SROCC | 0.8862 | 0.9157 | 0.8559 | 0.9248 |
| KRCC | 0.6907 | 0.7368 | 0.6559 | 0.7568 |
| RMSE | 10.2681 | 8.7385 | 10.9898 | 7.8572 |

This demonstrates that the proposed scheme is more stable across different distortion types, and well consistency with human perceptions. The result also indicates an indirect proof of the importance of binocular characteristics such as binocular combination in predicting the quality of stereoscopic images.

The scatter plots of objective scores (after logistic regression) versus subjective scores for each scheme are shown in Fig. 8, which are obtained by the following five-parameter logistic function [44], shown in Eq. (14). The vertical axis denotes the subjective ratings of the perceived distortions and the horizontal axis denotes the predicted objective scores.

$$DMOS = \beta_1 \times \left[\frac{1}{2} - \frac{1}{1 + \exp(\beta_2(x - \beta_3))} \right] + \beta_4 x + \beta_5 \quad (14)$$

where $\beta_1, \beta_2, \beta_3, \beta_4$ and β_5 are determined by using the subjective scores and the objective scores.

Referring to the results in Fig. 8, the scatter plot of the proposed scheme is more concentrated than other SIQA schemes, which indicates that the proposed framework is a useful predictor that can be effectively applied to predict the quality of stereoscopic images. Table 8 shows the MSE values associated to the regressions on scatter plots in Fig. 8, and the indicator highlighted in bold shows the best performance. Among all the models, our proposed model provides a consistent and outstanding performance, which further indicates that the proposed model can precisely predicts the quality of 3D images that contaminated by different types distortions.

Table 9 shows the time complexity comparison among the existed SIQA models. These SIQA models are implemented by MATLAB and the platform of Intel Core 2 Quad Q9500 2.83 GHz with 4 GB memory. Due to the need of disparity information, the

Table 9

Performance comparison between various 3D SIQA.

| Model | Benoit [10] | Chen [15] | Lin [16] | SDM-GSSIM |
|------------------|-------------|-----------|----------|-----------|
| Total time (min) | 442.39 | 345.94 | 3.04 | 61.6 |

model of Benoit and Chen take more time than other models. Although the model of Lin [16] spends the shortest time among these SIQA model, it has the worst overall performance which present in Table 7. In general, the proposed model is the most effective one to predict the quality of the stereoscopic images.

5. Conclusion

In this paper, a full-reference SIQA metric for stereoscopic images has been built with a clear advantage of less computing complexity and higher consistency with the subjective assessment for the symmetric distortions. The design of the framework is motivated by recent studies on the binocular combination behavior and the perception of symmetric distorted stereoscopic images. The proposed SDM-M metric tests on the LIVE 3D image quality Database, and the GSSIM-based model is significantly outperform conventional 2D-IQA models and well-known SIQA models.

An important contribution of this work is the demonstration that accounting for binocular combination behavior can greatly improve the performance of SIQA models. It assesses stereo images from the perspective of image quality and stereo sense based on Summation and Difference signals. From the experimental results, we find that the difference signals can be effectively used to estimate the depth perception in the proposed algorithm in the sense that a low computing complexity of SIQA performance is

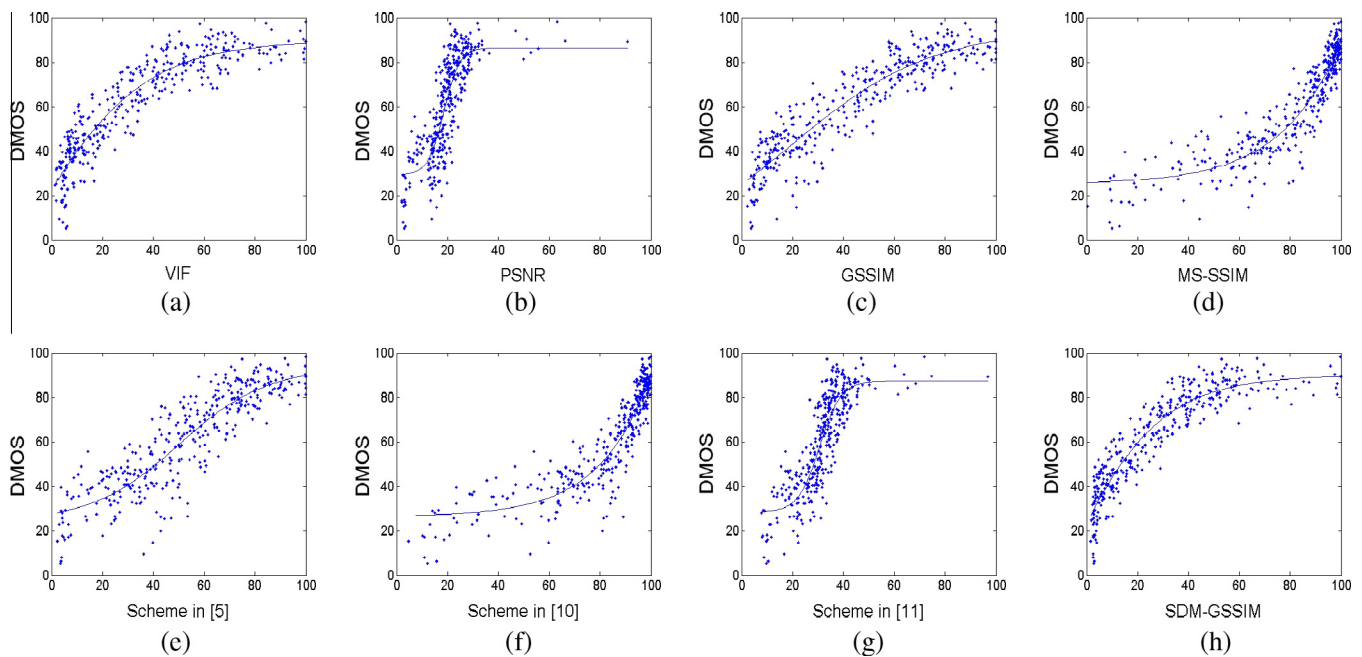


Fig. 8. Scatter plots of predicted objective scores versus DMOS for the eight schemes. (a) VIF. (b) PSNR. (c) GSSIM. (d) MS-SSIM. (e) Scheme in [10]. (f) Scheme in [15]. (g) Scheme in [16]. (h) Proposed scheme: SDM-GSSIM.

Table 8

MSE performance comparison.

| Model | VIF | PSNR | GSSIM | MS-SSIM | Benoit [10] | Chen [15] | Lin [16] | SDM-GSSIM |
|-------|---------|----------|---------|---------|-------------|-----------|----------|-----------|
| MSE | 69.1442 | 145.1543 | 74.6686 | 68.0394 | 105.4339 | 76.3614 | 120.7757 | 61.7356 |

maintained. What is more, the proposed metric can precisely predict the quality of the stereoscopic images that contaminated by different types of distortions. In the future work, the quality assessment method for stereo video, distorted by different types of distortions, will be the possible directions of our future work.

Acknowledgments

The authors would like to thank Prof. Alan C. Bovik for providing the LIVE 3D IQA Database. This research is partially supported by the National Natural Science Foundation of China (Nos. 61471260 and 61271324), and Program for New Century Excellent Talents in University (NCET-12-0400).

References

- [1] X.D. Zhang, X.C. Feng, W.W. Wang, W.F. Xue, Edge strength similarity for image quality assessment, *IEEE Sig. Process. Lett.* 20 (4) (2013) 319–322.
- [2] A. Tanchenko, Visual-PSNR measure of image quality, *J. Vis. Commun. Image Represent.* 25 (5) (2014) 874–878.
- [3] H. Yang, Y.M. Fang, Y. Yuan, W.S. Lin, Subjective quality evaluation of compressed digital compound images original research article, *J. Vis. Commun. Image Represent.* 26 (2015) 105–114.
- [4] Z. Wang, A.C. Bovik, H.R. Sheikh, E.P. Simoncelli, Image quality assessment: from eError visibility to structural similarity, *IEEE Trans. Image Process.* 13 (4) (2004) 600–612.
- [5] D.M. Chandler, S.S. Hemami, VSNR: a wavelet-based visual signal-to-noise-ratio for natural images, *IEEE Trans. Image Process.* 16 (2007) 2284–2298.
- [6] A. Maalouf, M.C. Larabi, CYCLOP: a stereo color image quality assessment metric, in: *IEEE International Conference on Acoustics, Speech and Signal Processing (ICASSP)*, 2011.
- [7] R. Bensalma, M.C. Larabi, A perceptual metric for stereoscopic image quality assessment based on the binocular energy, *Multidimens. Syst. Sig. Process.* 24 (2) (2013) 281–316.
- [8] W.A. Ijsselstein, H. de Ridder, J. Vliegen, Subjective evaluation of stereoscopic images: effects of camera parameters and display duration, *IEEE Trans. Circ. Syst. Video Technol.* 10 (2) (2000) 225–233.
- [9] J.S. Lee, L. Goldmann, T. Ebrahimi, Paired comparison-based subjective quality assessment of stereoscopic images, *Multim. Tools Appl.* (2012) 1–18.
- [10] A. Benoit, P. Le Callet, P. Campisi, P. Campisi, R. Cousseau, Quality assessment of stereoscopic images, *EURASIP J. Image Video Process.* 2008 (2008).
- [11] M. Lambooi, M. Fortuin, W.A. Ijsselstein, B.J. Evans, I. Heynderickx, Susceptibility to visual discomfort of 3-D displays by visual performance measures, *IEEE Trans. Circ. Syst. Video Technol.* 21 (12) (2011) 1913–1923.
- [12] D. Kim, K. Sohn, Visual fatigue prediction for stereoscopic image, *IEEE Trans. Circ. Syst. Video Technol.* 21 (2) (2011) 231–236.
- [13] W. Chen, J. Fournier, M. Barkowsky, P. Le Callet, Quality of experience model for 3DTV, *Int. Soc. Optics Photon.* 8288 (2012).
- [14] F. Shao, W.S. Lin, S.B. Gu, G.Y. Jiang, T. Srikanthan, Perceptual full-reference quality assessment of stereoscopic images by considering binocular visual characteristics, *IEEE Trans. Image Process.* 22 (5) (2013) 1940–1953.
- [15] M.J. Chen, C.C. Su, D.K. Kwon, L.K. Cormack, A.C. Bovik, Full-reference quality assessment of stereopairs accounting for rivalry, *Sig. Process.: Image Commun.* 28 (9) (2013) 1143–1155.
- [16] Y.H. Lin, J.L. Wu, Quality assessment of stereoscopic 3D image compression by binocular integration behaviors, *IEEE Trans. Image Process.* 23 (4) (2014) 1527–1542.
- [17] Y. Zhao, Z.Z. Chen, C. Zhu, Y.P. Tan, L. Yu, Binocular just-noticeable-difference model for stereoscopic images, *IEEE Sig. Process. Lett.* 18 (1) (2011) 19–22.
- [18] S.W. Jung, S.J. Ko, Depth map based image enhancement using color stereopsis, *IEEE Sig. Process. Lett.* 19 (5) (2012) 303–306.
- [19] P. Hanhart, T. Ebrahimi, Subjective evaluation of two stereoscopic imaging systems exploiting visual attention to improve 3D quality of experience, in: *Proceedings of SPIE 9011, Stereoscopic Displays and Applications XXV*, 90110D, 2014.
- [20] Z. Lv, T. Su, 3D Seabed Modeling and Visualization on Ubiquitous Context, *SIGGRAPH Asia 2014 Posters*, ACM, 2014.
- [21] Z. Lv, X. Li, B. Zhang, W. Wang, S. Feng, J. Hu, Big city 3D visual analysis, in: *Eurographics2015. European Association for Computer Graphics*, 2015.
- [22] K. Zeng, Z. Wang, 3D-SSIM for video quality assessment, in: *2012 19th IEEE International Conference on Image Processing (ICIP)*, September 30 2012–October 3 2012, pp. 621–624.
- [23] J.P. López, J.A. Rodrigo, D. Jiménez, J.M. Menéndez, Stereoscopic 3D video quality assessment based on depth maps and video motion, *EURASIP J. Image Video Process.* 2013 (1) (2013) 1–14.
- [24] C.T. Tsai, H.M. Hang, Quality assessment of 3D synthesized views with depth map distortion, *Vis. Commun. Image Process. (VCIP)* (2013) 1–6.
- [25] E. Bosc, F. Battisti, M. Carli, P. Le Callet, A wavelet-based image quality metric for the assessment of 3D synthesized views, in: *Proceedings of SPIE 8648, Stereoscopic Displays and Applications XXIV*, 86481Z, 2013.
- [26] Q. Jiang, F. Duan, F. Shao, 3D visual attention for stereoscopic image quality assessment, *J. Softw.* 9 (7) (2014).
- [27] F. Battisti, E. Bosc, M. Carli, P. Le Callet, S. Perugia, Objective image quality assessment of 3D synthesized views, *Sig. Process.: Image Commun.* 30 (2015) 78–88.
- [28] J. Park, H. Oh, S. Lee, A.C. Bovik, 3D visual discomfort predictor: analysis of horizontal disparity and neural activity statistics, *IEEE Trans. Image Process.* 24 (3) (2015) 1101–1114.
- [29] I.P. Howard, B.J. Rogers, *Binocular Vision and Stereopsis*, Oxford University Press, New York, 1995.
- [30] W.J.M. Levelt, *On Binocular Rivalry*, Mouton, The Hague, The Netherlands, 1968.
- [31] A.I. Cogan, Human binocular interaction: towards a neural model, *Vis. Res.* 27 (12) (1987) 2125–2139.
- [32] S. Grossberg, F. Kelly, Neural dynamics of binocular brightness perception, *Vis. Res.* 39 (22) (1999) 3796–3816.
- [33] H.R. Silva, S.H. Bartley, Summation and subtraction of brightness in binocular perception, *Brit. J. Psychol. Gen. Sec.* 20 (3) (1930) 241–250.
- [34] Z. Li, J.J. Atick, Efficient stereo coding in the multiscale representation, *Netw.: Comput. Neural Syst.* 5 (2) (1994) 157–174.
- [35] F.A.A. Kingdom, Binocular vision: the eyes add and subtract, *Curr. Biol.* 22 (1) (2012) R22–R24.
- [36] N. Yun, Z.Y. Feng, J.C. Yang, J.J. Lei, The objective quality assessment of stereo image, *Neurocomputing* 120 (23) (2013) 121–129.
- [37] N. Qian, S. Mikaelian, Relationship between phase and energy methods for disparity computation, *Neural Comput.* 12 (2) (2000) 279–292.
- [38] L. Zhang, L. Zhang, X. Mou, D. Zhang, FSIM: a feature similarity index for image quality assessment, *IEEE Trans. Image Process.* 20 (8) (2011) 2378–2386.
- [39] J.J. Atick, A.N. Redlich, What does the retina know about natural scenes?, *Neural Comput.* 4 (4) (1992) 196–210.
- [40] H.R. Sheikh, A.C. Bovik, Image information and visual quality, *IEEE Trans. Image Process.* 15 (2) (2006) 430–444.
- [41] G.H. Chen, C.L. Yang, S.L. Xie, Gradient-based structural similarity for image quality assessment, in: *IEEE International Conference on Image Processing*, 2006, pp. 2929–2932.
- [42] Z. Wang, E.P. Simoncelli, A.C. Bovik, Multi-scale structural similarity for image quality assessment, in: *2004 Conference Record of the Thirty-Seventh Asilomar Conference on Signals, Systems and Computers*, vol. 2, 2003, pp. 1398–1402.
- [43] A.K. Moorthy, C.C. Su, A. Mittal, A.C. Bovik, Subjective evaluation of stereoscopic image quality, *Sig. Process.: Image Commun.* 28 (8) (2013) 870–883.
- [44] P.G. Gottschalk, J.R. Dunn, The five-parameter logistic: a characterization and comparison with the four-parameter logistic, *Anal. Biochem.* 343 (1) (2005) 54–65.